Available online at www.eccomasproceedia.org
Eccomas Proceedia COMPDYN (2023) 1744-1757

ECCOMAS
Proceedia

COMPDYN 2023
9th ECCOMAS Thematic Conference on
Computational Methods in Structural Dynamics and Earthquake Engineering
M. Papadrakakis, M. Fragiadakis (eds.)
Athens, Greece, 12-14 June 2023

ON THE IN-PLANE FLEXURAL RESPONSE OF CANTILEVER UNREINFORCED CLAY BRICKWORK MASONRY WALL PANELS

Hisham Tariq[1], Mohammad Amir Najafgholipour[2], Vasilis Sarhosis[3] and Gabriele Milani [4]

[1] Department of Civil Infrastructure and Environmental Engineering, Khalifa University, Abu Dhabi 127788, UAE
e-mail: 100063744@ku.ac.ae

[2] Department of Civil and Environmental Engineering, Shiraz University of Technology, Shiraz, Iran
e-mail: najafgholipour@sutech.ac.ir

[3] School of Civil Engineering, University of Leeds, Leeds, LS2 9JT, UK
e-mail: V.Sarhosis@leeds.ac.uk

[4] Department of Architecture, Built Environment and Construction Engineering (ABC), Politecnico di Milano, Piazza Leonardo da Vinci 32, 20133 Milan, Italy
e-mail: gabriele.milani@polimi.it

Abstract

This paper studies the in-plane response of unreinforced clay brickwork masonry wall panels. For this purpose, a non-linear three-dimensional heterogenous Finite Element (FE) model was developed using ABAQUS software. The model was validated against experimental studies obtained from the literature. Then, a parametric study was undertaken to investigate the effects of a) pre-compression, b) Height to Length ratio (H/L) of the wall and c) H/L of the masonry units on the in-plane strength, initial stiffness, peak drift and ultimate drift limit. Finally, results obtained from the FE computational models compared against those obtained from design codes (Eurocode) for determining the in-plane force capacity and drift capacity of the URM walls. From the analysis of results it was found that in most cases, Eurocode overestimates the ultimate drift ratio when compared to the findings from the FE analyses.

Keywords: Unreinforced masonry, simplified micro modelling, numerical modelling, code formulations.

ISSN:2623-3347
Peer-review under responsibility of the organizing committee of COMPDYN 2023.
doi: 10.7712/120123.10516.20980

1 INTRODUCTION

Masonry is characterized by its ability to withstand high compressive stresses than tensile ones. It is the mortar joint in a masonry wall panel which acts as a plane of weakness. Failure in masonry wall panels depends among others on the material properties of bricks and mortar, boundary conditions of the wall e.g., pre-compression levels applied on the wall, Height to Length (H/L) ratio of the wall, H/L ratio of the masonry units etc. Typical failure mechanisms in masonry wall panels include rocking, toe-crushing, sliding and diagonal tension failure. Over the years, several studies investigated the in-plane response of masonry walls using experimental tests, analytical methods and numerical models [1-5]. In this paper, code formulations provided in Eurocode [6-9] for calculating the in-plane force capacity and drift ratio are compared against results obtained from analytical and high-fidelity models. In particular, three different URM wall configurations (with varying H/L ratio of the wall) were considered herein. Initially, the high-fidelity model developed based on the three dimensional FE software Abaqus and validated against experimental test results found in the literature. The validated FE model was then used into a parametric study where the H/L ratio of the wall, H/L ratio of bricks and pre-compression of the wall were varied. A comparison between the findings obtained from analytical models and FE analysis is also presented.

2 CODE FORMULATIONS FOR IN-PLANE RESPONSE OF URM WALLS

In this section, summary of code formulations for quantifying in-plane response (in-plane strength, elastic stiffness, and drift) of URM walls are summarized.

2.1 Stiffness

Eq. (1) gives the estimate of the elastic stiffness (K_{el}) of the wall determined by considering elastic beam theory [10,11].

$$K_{el} = \frac{1}{\frac{h^3}{\alpha_K E_m I} + \frac{h}{A_n G_m}} \tag{1}$$

where 'h' is the height of the wall, 'E_m' is the Young's Modulus of masonry ($E_m = 550 f_m$) and 'G' is shear modulus given by G_m = 0.4 E_m [6]. Area moment of inertia, $I = tl^3/12$, 'l' and 't' are length and thickness of the wall respectively. $A_n = lt$ is the cross-sectional area of the wall while α_K is a parameter that changes depending on the geometric boundary conditions of the wall ($e.g.$, α_K = 0.83 for fixed-fixed walls and α_K = 3.33 for cantilever walls).

2.2 In-plane strength according to Eurocode

Eurocode identifies three failure modes for URM walls under in-plane loading: flexural failure (toe-crushing), sliding failure, and diagonal shear failure. In-plane strength formulations corresponding to different modes of failure are shown in equations (2) to (4):

1- Flexural toe-crushing (V_f):

$$V_f = \frac{N \cdot l}{2 \cdot h_0}\left(1 - \frac{N}{0.87 \cdot l \cdot t \cdot f_m}\right) \tag{2}$$

where 'N' is the pre-compression load, 'h_0' is the shear span measured from wall base ($h_0 = h$ for cantilever condition and $h_0 = h/2$ for fixed-fixed condition), and 'f_m' is the compressive strength of masonry.

2- Sliding failure (V_{sl}):

$$V_{sl} = f_{vk} \cdot t \cdot l' \tag{3}$$

where 'l'' is the length of the compressed part of the wall, which depends on the eccentricity 'e'. For this study, e = 0 and hence $l' = l$. The characteristic shear strength of the masonry 'f_{vk}' should be less than or equal to 6.5 % of brick compressive strength. It is a function of cohesion of masonry 'f_{vk0}' and pre-compression 'σ_0' and is given as:

$$f_{vk} = \begin{cases} f_{vk0} + 0.4\sigma_0 & ;if\ bed\ and\ head\ joints\ are\ fully\ filled\ with\ mortar \\ 0.5f_{vk0} + 0.4\sigma_0 & ;if\ vertical\ joints\ are\ not\ filled\ with\ mortar \end{cases}$$

3- Diagonal Tension (V_{dt}):

$$V_{dt} = \frac{t \cdot l}{b} f_t \sqrt{1 + \frac{\sigma_0}{f_t}} \tag{4}$$

where 'f_t' is the tensile strength of masonry obtained from experiments and 'b' is a shape correction factor ($1.0 \leq b = h/l \leq 1.5$). In this paper, URM walls with same thickness (t = 150 mm) and three different H/L ratios were studied (see Table 1). Material properties used in this study are summarized in Table 2. Fig. 1 shows the dependence of the in-plane strength ON pre-compression computed using the above-mentioned equations for all three URM walls.

H/L	0.48	0.96	1.44
Height (mm)	2600	2600	2600
Length (mm)	5400	2700	1800

Table 1: Geometric properties of different URM walls studied in this paper

E_m (MPa)	f_m (MPa)	f_t (MPa)	f_{vk0} (MPa)
3190	5.80	0.50	0.26

Table 2: Material parameters of masonry used for the analytical study.

2.3 Limiting drift ratio according to Eurocode

The drift limits Δ_u and Δ_{u2} corresponding to significant damage and near collapse limit states respectively are prescribed by Eurocode.

For walls whose failure is governed by flexural mechanisms, $\Delta_{Fu} = 0.01(1 - N/ltf_m) \times \Delta_{Fu2}$ is the drift corresponding to 10% drop in shear force for regular masonry given by $\Delta_{Fu2} = 1.33 \times \Delta_{Fu}$. For shear sliding failure, Δ_{Su} equal to 0.5 % is suggested when masonry unit strength limits the sliding. Also, the residual shear strength corresponding to Δ_{Su2} ($1.33 \times \Delta_{Su}$) can be obtained from Eq. (3), without considering cohesion (f_{vk0}). Ultimate drift, Δ_{Du} = 0.6%

is suggested for walls failing in diagonal shear with a drop of 50 % in shear force at Δ_{Du2} ($1.33 \times \Delta_{Du}$) for regular masonry.

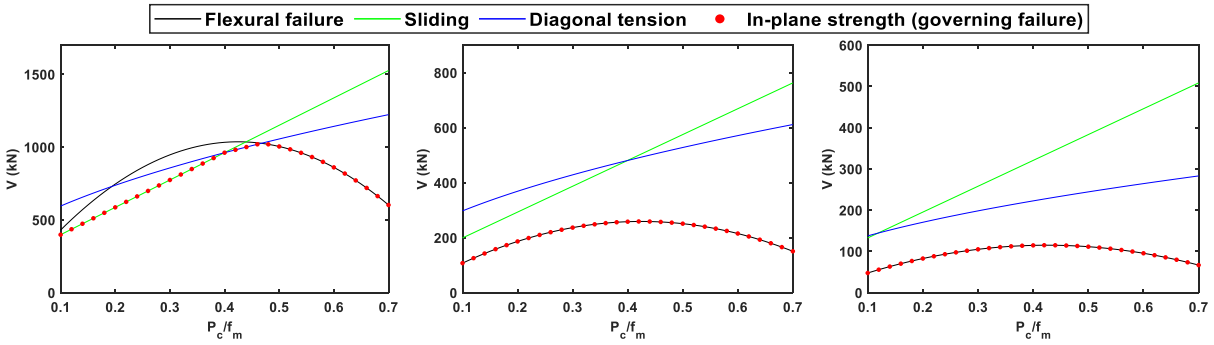

Squat wall (H/L = 0.48) Square wall (H/L = 0.96) Slender wall (H/L = 1.44)

Figure 1: In-plane shear capacity of URM walls according to Eurocode.

3 FINITE ELEMENT MODELLING AND VALIDATION

Numerical modeling provides an effective platform for investigating the structural response of engineering systems at a fraction of the cost of experiments. Modelling approaches for studying the behaviour of masonry structures based on finite element method include (i) macro-modelling [12,13] (ii) simplified micro-modelling [14,15] and (iii) detailed micro-modelling [16,17,18,19]. In this paper, a simplified micro-modelling approach based on cohesive elements and a VUMAT subroutine was implemented in Abaqus 2021 to model URM walls. Extended masonry units were modelled as linear brick elements with reduced integration whereas cohesive elements (COH3D8) were employed to simulate the mortar joints and potential brick cracks. Concrete damage plasticity model was used to simulate the material behaviour of masonry units and cohesive behaviour of joints was simulated using a VUMAT subroutine. For detailed explanation of FE modelling and material parameters, the reader can refer to [20].

3.1 Validation of the FE model

The finite element model was validated against a quasi-static reverse cyclic test of a URM wall (T1 wall) performed at ETH Zurich [5]. The wall was made of perforated clay bricks with size 290 × 150 × 190 mm^3. Material properties used in the validation of the finite element model and the parametric study are presented in Table 3 and 4 accordingly. A pre-compression equal to 10 % of masonry compressive strength was applied on the wall followed by a reverse cyclic in-plane drift under shear controlled conditions. FE results are in good agreement with the experimental results in terms of damage contours and load-displacement response (see Fig. 2 and 3). Furthermore, T7 wall (same as T1 wall but with cantilever boundary conditions), also corresponds well with FE results, as experimental in-plane strength (V_{EXP}) of T7 wall is 108 kN and V_{FEM} is 112 kN.

3.2 Parametric Study

The validated FE model with a converged mesh size of 75 mm × 75 mm × 100 mm was employed for a parametric study. In this paper, three different H/L ratios of single leaf URM walls were considered (as mentioned in Section 2.2, Table 1) and pre-compression was varied from 0.10f_m to 0.70f_m with intervals of 0.05f_m. Finally, two different H/L ratios of masonry

unit (H/L = 0.655: H = 190 mm, L = 290 mm and H/L = 0.310: H = 90 mm, L = 290 mm) were considered in this study.

E_{brick} (MPa)	10520	Dilation Angle (ψ)	31^O
Density (kg/m^3)	2400	Eccentricity (ε)	0.1
Poisson's Ratio	0.15	σ_{b0}/σ_{c0}	1.16
f_m (MPa)	5.80	K_c	0.67
$f_{t,brick}$ (MPa)	1.27	Viscosity Parameter	0

Table 3: Material properties of masonry used in FEM.

Parameter	Horizontal Joints	Vertical Joints	Brick cracks
f_t (MPa)	0.138	0.0375	1.27
G_f^1(N/mm)	0.125	0.034	0.107
c (MPa)	0.26	0.07	1.91
Tan(ϕ)	0.94	0.94	0.75
G_f^2 (N/mm)	1.25	0.34	1.07
k_n (N/mm^3)	28.9	7.81	400
$k_{sx,y}$ (N/mm^3)	5.93	1.62	400
κ_1/κ_t	0.76	0.76	0.76

Table 4: Material properties of the interface elements.

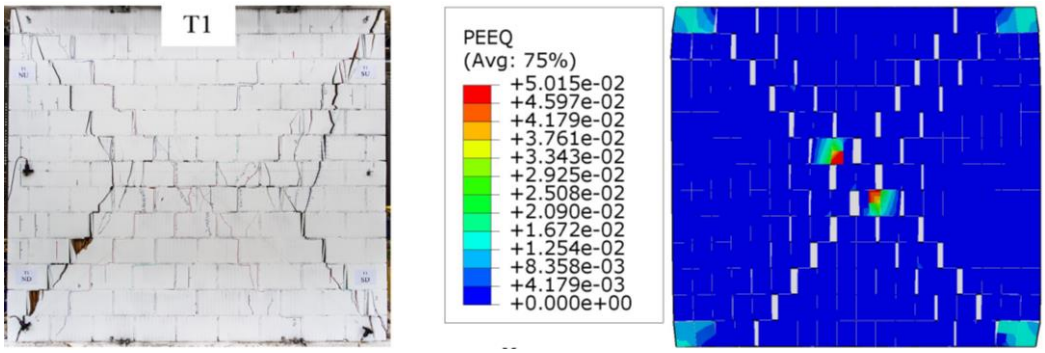

Figure 2: Damage patterns from experimental tests and finite element analysis.

4 NUMERICAL RESULTS FROM THE FINITE ELEMENT ANALYSIS

Flexural failure mechanisms were observed for the URM walls simulated using FEM. Particularly, slender (H/L = 1.44) and square (H/L = 0.96) walls failed in rocking followed by toe-crushing for low intensities of pre-compression, whereas higher pre-compression resulted in toe-crushing failure mode. Hybrid failure mechanisms (i.e., a combination of diagonal sliding and flexure failure) were observed for squat walls under low pre-compression, whereas toe-crushing was seen in squat walls under high pre-compression. In [20], an extensive investigation and discussion of the failure mechanisms of such walls and their dependence on the pre-compression, height to length ratio of the wall and height to length ratio of bricks is presented

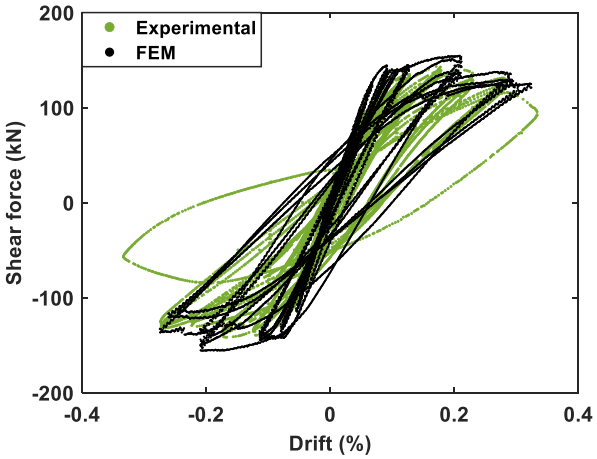

Figure 3: Load vs drift curves from experiments and FEM.

For studying the in-plane response of flexure controlled URM walls, in-plane strength V_u, numerical stiffness K_{num} (secant stiffness evaluated at 10–40% of in-plane strength), drift ratio corresponding to in-plane strength Δ_{peak} and the ultimate drift ratio Δ_u (drift ratio at 80% of the in-plane strength in post peak region) were considered. A discussion on the influence of pre-compression, height to length ratio of the wall and height to length ratio of the masonry units on these parameters follows.

4.1 In-plane strength

From the FE findings, it was shown that the in-plane strength of the wall increases as H/L ratio of the wall decreases. This trend still existed if the in-plane strength in unit length of the wall was considered, see Fig. 4. Pre-compression strongly affected the in-plane strength of the walls. For all walls, the in-plane strength would increase initially as pre-compression increased, peak at P_c values between 30% and 45% of masonry compressive strength, and then begin to decline as illustrated in Fig. 4. Furthermore, numerical results demonstrated that as the H/L ratio of the wall decreases, the in-plane force capacity becomes more sensitive to the pre-compressive stress. Hence, the effect of pre-compression and height to length ratio of the wall on its in-plane strength can be interdependent, meaning that for the walls with lower H/L ratio same increase of pre-compression can result in a greater increment of in-plane strength than the wall with higher H/L ratio. In-plane strength was found to be very less sensitive to height to length ratio of the masonry units for square and slender walls whereas for squat walls H/L ratio of bricks had some effect on the in-plane strength as shown in Fig. 4 (a).

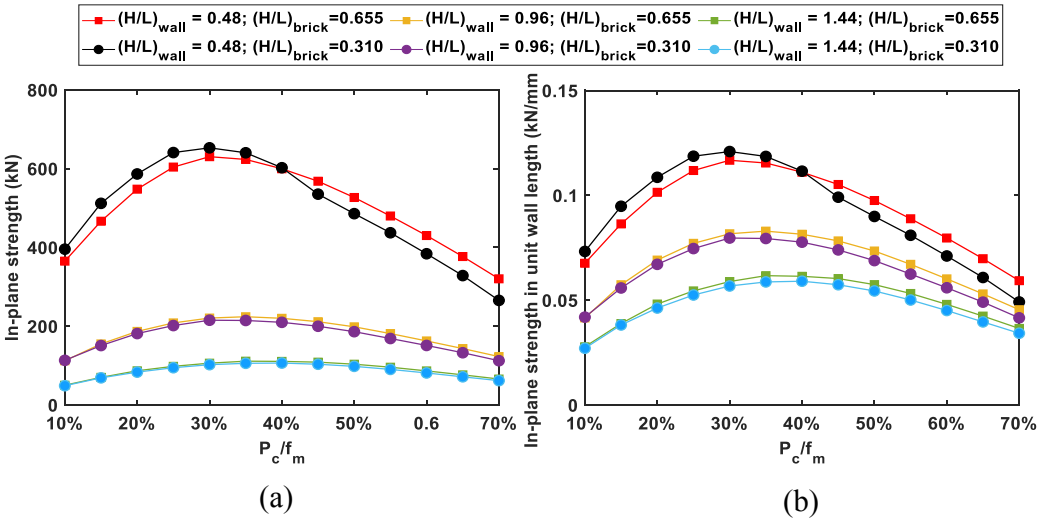

Figure 4: In-plane strength in relation with pre-compression for different H/L ratios of wall and two H/L ratios of bricks (a) In-plane strength (kN) (b) In-plane strength in unit wall length (kN/mm)

4.2 Stiffness (K_{num})

As expected, increase in the numerical stiffness of the wall (calculated at 10% of in-plane strength) was observed as H/L ratio of the wall decreased, as lower H/L ratio corresponds to higher area moment of inertia of the wall (see Fig. 5). Also, pre-compression does not seem to have any considerable effect on the numerical stiffness of the URM wall as shown in Fig. 4 and supported by the results [15,21]. The mean change in numerical stiffness for all the walls caused by the variation of pre-compression from 10% to 70% of masonry compressive strength is 7%. Slender walls (H/L = 1.44) and $(H/L)_{brick}$ = 0.655 show maximum change in the stiffness due to the variation of pre-compression, which is 11.8%. H/L ratio of masonry units significantly affected the stiffness, with bricks having lower H/L ratio yielding lower wall stiffness (Fig. 5). A lower H/L ratio of bricks results in a greater number of bricks and mortar joints inside the wall, which results in a greater degree of anisotropy and a subsequent reduction in the stiffness of the wall.

4.3 Drift corresponding to peak load (Δ_{peak}) and ultimate drift ratio (Δ_u)

Pre-compression, height to length ratio of the wall, and height to length ratio of the bricks were found to affect both Δ_{peak} and Δ_u. With increase in pre-compression, Δ_{peak} as well as Δ_u decreased with an exception of squat wall with $P_c = 0.15f_m$ and $(H/L)_{brick}$ = 0.312 (see Fig. 6 and 7). This particular wall configuration deviated from the trend and Δ_u at $P_c = 0.15f_m$ is higher than Δ_u at $P_c = 0.10f_m$. A hybrid failure, which involves both rocking and sliding followed by toe-crushing, was observed in squat walls at low levels of pre-compressive stresses. Additionally, height to length ratio of the brick have a significant impact on the shear failure mechanism. Bricks with smaller H/L ratio tend to resist the diagonal sliding failure [20] and it causes failure in the form of vertical cracks passing through bricks and head joints. As a result, there may be a need for a greater amount of drift in order to cause 80% drop in shear force in this case which explains the deviation in the trends of ultimate drift ratio.

In general, it was observed that Δ_{peak} increases with an increase in the H/L ratio of the wall with a slight variation in squat walls with $(H/L)_{brick}$ = 0.310 under pre-compression (0.15 - 0.25)f_m. Also, the walls having bricks with lower H/L ratio had low Δ_{peak} (see Fig. 6). Ultimate drift ratio showed strong dependence on height to length ratio of the wall as well as H/L ratio

of the bricks. Squat walls with high $(H/L)_{brick}$ exhibited higher ultimate drift ratio for pre-compression levels varying from 10% to 25% of masonry compressive strength, see Fig. 7 (a).

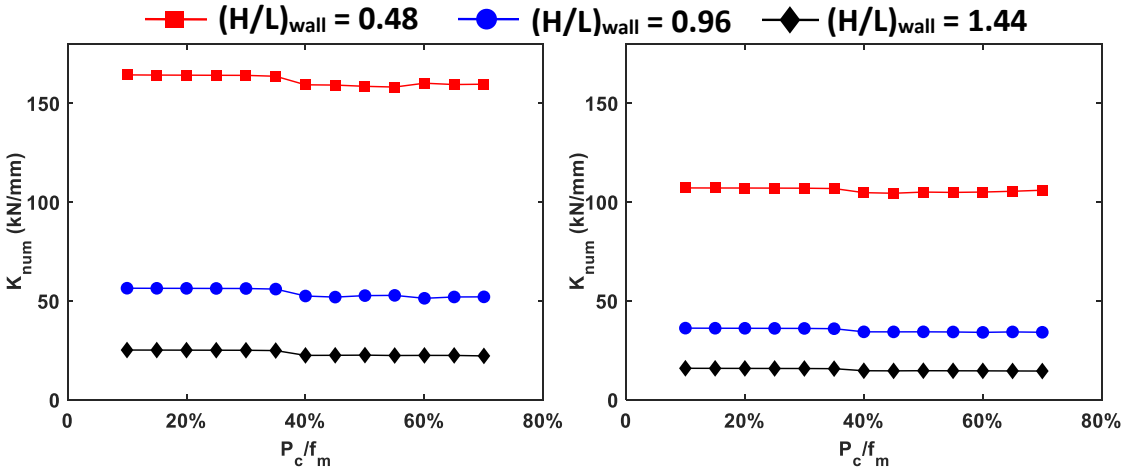

Figure 5: Variation of numerical stiffness (K_{num}) with pre-compression for URM walls with different H/L ratios (a) $(H/L)_{brick}$ = 0.655 (b) $(H/L)_{brick}$ = 0.310

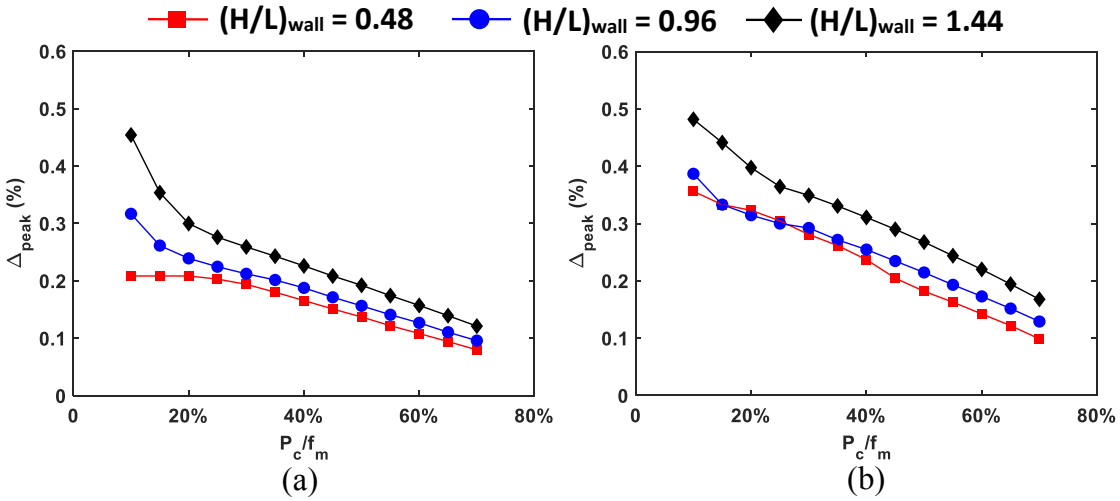

Figure 6: Variation of drift ratio corresponding to peak load (Δ_{peak}) with pre-compression for URM walls with different H/L ratios (a) $(H/L)_{brick}$ = 0.655 (b) $(H/L)_{brick}$ = 0.310

Ductility in the post-peak region can be assessed by the ratio Δ_u/Δ_{peak} , see Fig. 8. When this ratio is equal to one, it implies brittle failure; nevertheless, as it grows, it also indicates an increase in the ductility in the post-peak region. Δ_u/Δ_{peak} showed very different trends depending on the height to length ratio of the bricks. For $(H/L)_{brick}$ = 0.655, Δ_u/Δ_{peak} was almost equal to one for slender and square walls under all pre-compression levels indicating a brittle post peak behaviour, but higher values of Δ_u/Δ_{peak} for squat walls under low pre-compression ($0.1f_m$ – $0.25f_m$) implied a relatively ductile post peak region. For lower $(H/L)_{brick}$ = 0.312, slender and square walls demonstrated some post peak ductility for P_c = ($0.10f_m$ -$0.25f_m$) and higher pre-compression caused brittle failure whereas squat walls showed post peak ductility only for P_c = ($0.10f_m$ and $0.15f_m$).

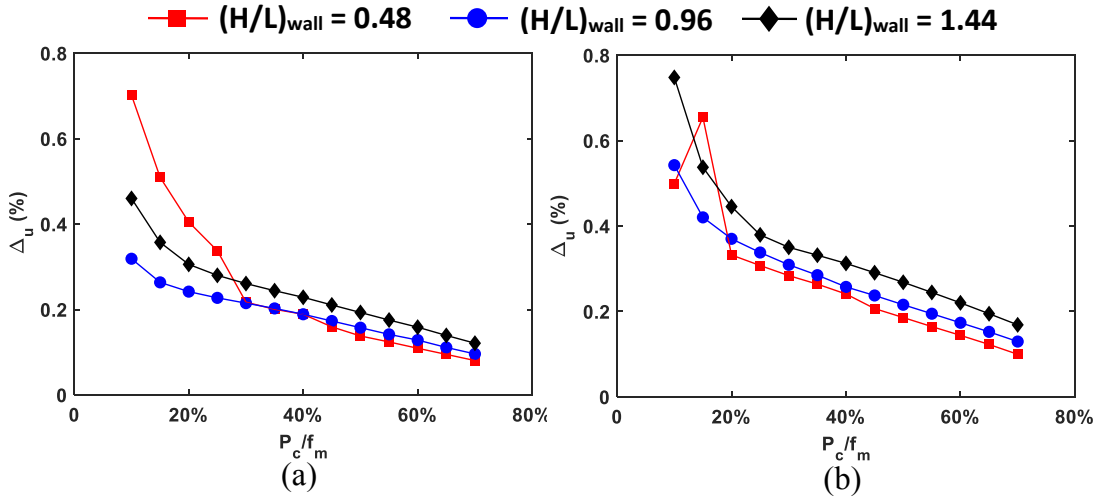

Figure 7: Variation of ultimate drift ratio (Δ_u) with pre-compression for URM walls with different H/L ratios (a) $(H/L)_{brick}$ = 0.655 (b) $(H/L)_{brick}$ = 0.310

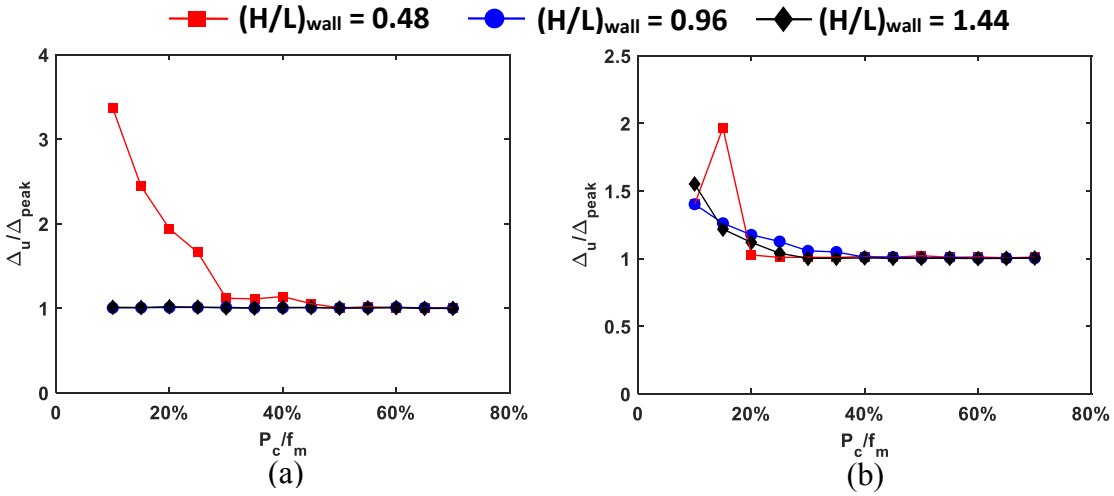

Figure 8: Variation of (Δ_u/Δ_{peak}) with pre-compression for URM walls with different H/L ratios (a) $(H/L)_{brick}$ = 0.655 (b) $(H/L)_{brick}$ = 0.310

5 COMPARATIVE ASSESSMENTS WITH CODES OF PRACTICE

In this section, the results that were produced via numerical modeling are compared with the results that were obtained from the design code formulations.

5.1 Stiffness

The comparison between numerical stiffness (K_{num}) and elastic stiffness is presented in Fig. 9. Since pre-compression has no significant influence on the numerical stiffness, the mean of the numerical stiffnesses at different pre-compressive stress values is shown in Fig. 9. The stiffness of the URM wall was significantly overestimated by Eq. (1), and this finding has been reported in the literature [22,23]. The reason for this overestimation is the anisotropic behaviour of the masonry which is not taken into account by Eq. (1). Numerical stiffness (K_{num}) was found to be, on average, 52 % of the stiffness calculated using the elastic beam theory. The effective stiffness is typically in the range of 40-80% of the elastic stiffness as indicated in the literature

[15,24]. Assuming that K_{num} is the effective stiffness, K_{num} is within the abovementioned range (0.4-0.8 K_{el}) for most of the cases as shown in Fig. 9.

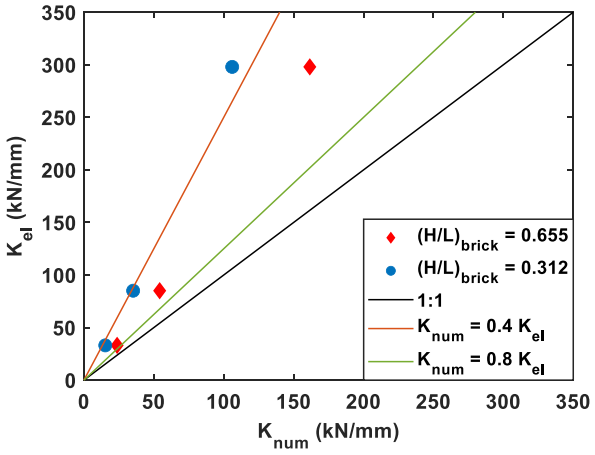

Figure 9: Comparison of stiffness obtained from numerical modelling and elastic beam theory for different URM wall configurations.

5.2 In-plane strength

Fig. 10 compares the in-plane strengths calculated from Eurocode equations and FE modeling (H/L of brick = 0.655) for different walls subjected to varying intensities of pre-compression. It can be observed that the analytical relations and FE results are in good agreement for slender walls (H/L = 1.44) for all levels of pre-compression. For square walls (H/L = 0.96), Eurocode relations predict the in-plane strength with good accuracy for pre-compression levels ($0.10f_m$ - $0.25f_m$) whereas certain overestimation by Eurocode can be observed for these walls under pre-compression levels ($0.30f_m$ -$0.70f_m$). A very significant overestimation of in-plane strength can be observed for squat walls (H/L = 0.48) especially for pre-compression ($0.25f_m$ - $0.70f_m$). Similar discrepancy between the in-plane strengths determined from FE analyses and analytical formulations (ASCE 41-17 and Italian Code) was reported by [1]. The design codes do not consider a possibility of the occurrence of the combined failure (rocking and diagonal shear failure). Furthermore, the reduction factor, κ (= 0.87 in Eurocode, 0.7 in ASCE 41-17 and 0.85 in Italian Code) in the toe-crushing relation is defined just to idealize the constant distribution of the compressive stresses at the base of the wall and it does not take into account the height to length ratio of the wall and the constraint conditions. These two factors can be attributed to this huge difference between the results from numerical simulations and analytical formulations.

5.3 Load-drift curves

Load-drift (P-Δ) curves are represented as piecewise linear curves using the formulations discussed in section 2. In the elastic region, a bilinear relationship is assumed in which $P = K_{el} \times \Delta$ is assumed till $0.7V_u$ and 50% reduction in K_{el} is considered for the second part of the elastic region up to yield drift (Δ_y). A zero slope is assumed between Δ_y and Δ_u followed by reduction in shear force at Δ_{u2} according to the failure mode. Fig. 11 shows the comparison of load-drift curves obtained from FE modelling and analytical equations. Clearly, H/L ratio of the bricks have a significant influence on the in-plane response of the URM wall panels. Furthermore, the revised version of Eurocode overestimated the drift capacities for almost all the cases. This is partly because most of the code equations are proposed based on the experimental

tests on solid brick walls which tend to have high drift capacities [5,25]. A good agreement between FE results and code equations was found in terms of in-plane force capacity for low levels of pre-compression (10-20 % of masonry compressive strength) only and the deviation between the results increased with decrease in H/L ratio.

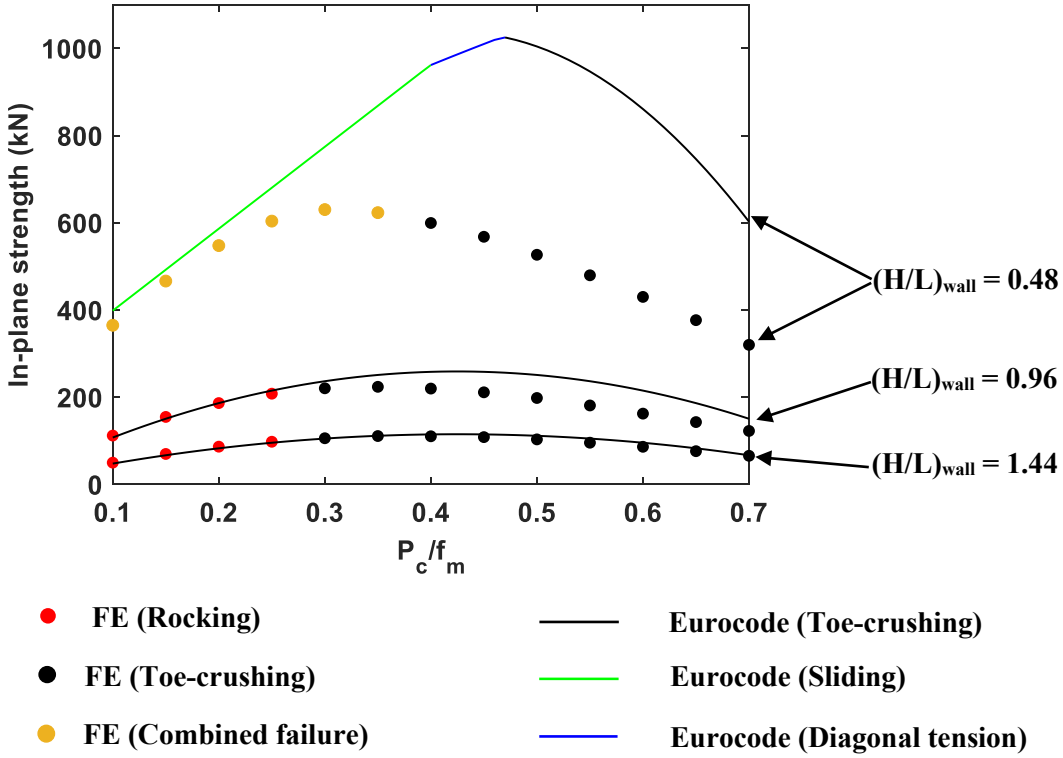

Figure 10: Comparison of in-plane strengths obtained from numerical modelling and Eurocode formulations for different URM wall configurations.

6 CONCLUSIONS

This paper presents the numerical investigation of URM walls under in-plane shear with focus on cantilever (fixed-free) boundary conditions. A 3D FE model developed in ABAQUS is implemented in an extensive parametric study to investigate the influence of pre-compression, height to length ratio of the wall and height to length ratio of the bricks on the in-plane response of URM walls. Additionally, a summary of analytical relations given in Eurocode for quantifying the in-plane behaviour of URM walls in terms of in-plane strength and drift ratio is also presented. A comparison of results obtained from FE analyses and code provisions is also presented.

In most cases, Eurocode overestimates the ultimate drift ratio when compared to the findings of FE analyses. In-plane strength is also overestimated by Eurocode except at low levels of pre-compression ($0.1f_m – 0.2f_m$). A very huge disparity between the results of design codes and FE analyses can be seen in case of squat walls (H/L = 0.48).

Analytical models determining the drift ratio can incorporate normalized pre-compression, H/L ratio of the wall and the geometric boundary conditions. Furthermore, an extensive experimental study on the perforated URM walls, particularly squat walls, is suggested to better quantify the in-plane response of the walls.

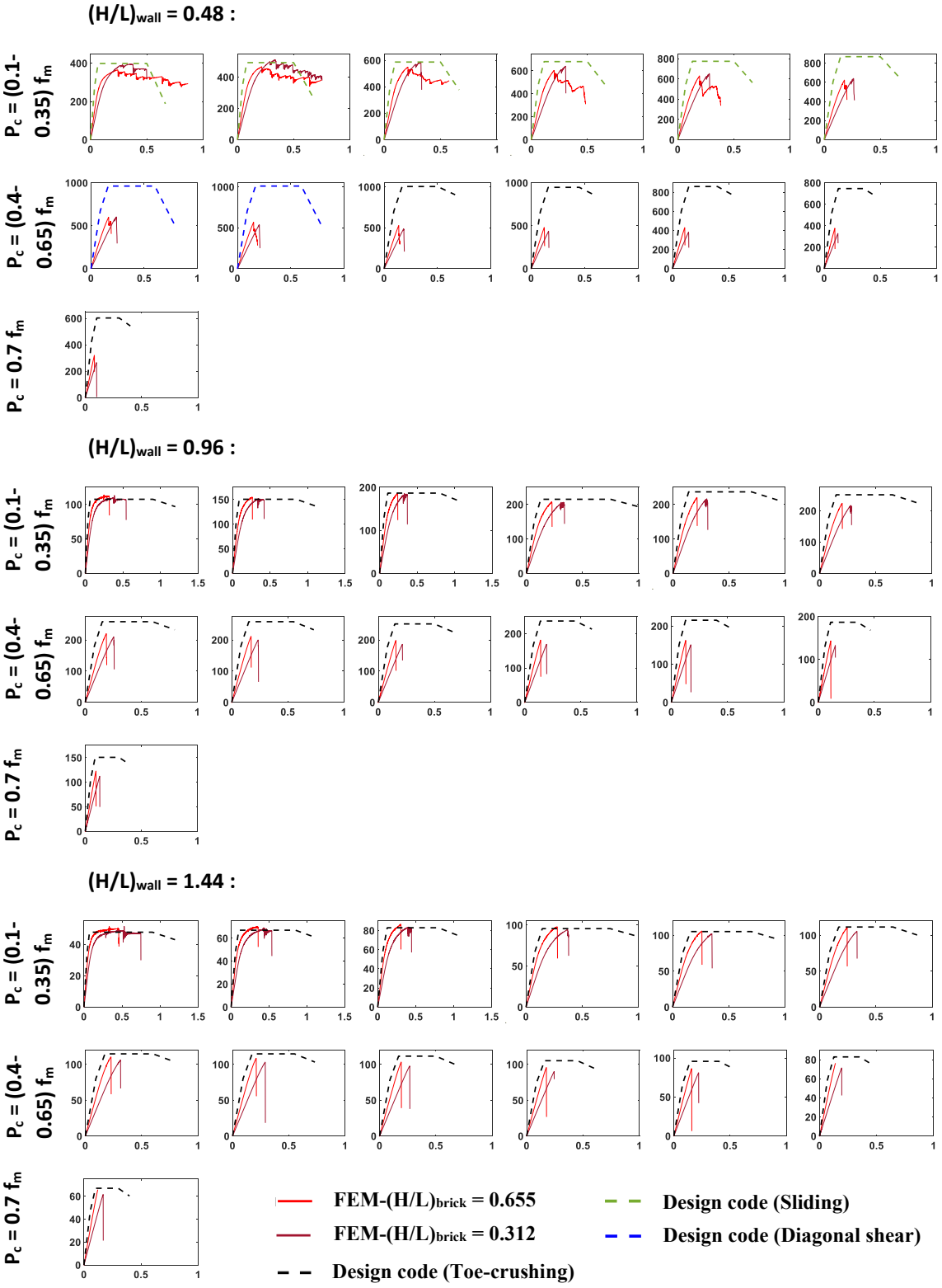

Figure 11: Comparison of Load vs drift curves obtained from FEA and design code formulations.

REFERENCES

[1] Petry, S., & Beyer, K. (2015). Cyclic test data of six unreinforced masonry walls with different boundary conditions. Earthquake Spectra, 31(4), 2459-2484.

[2] Haach, V. G., Vasconcelos, G., & Lourenço, P. B. (2011). Parametrical study of masonry walls subjected to in-plane loading through numerical modeling. Engineering Structures, 33(4), 1377-1389.

[3] D'Altri, A. M., Sarhosis, V., Milani, G., Rots, J., Cattari, S., Lagomarsino, S., ... & de Miranda, S. (2020). Modeling strategies for the computational analysis of unreinforced masonry structures: review and classification. Archives of computational methods in engineering, 27(4), 1153-1185.

[4] Celano, T., Argiento, L. U., Ceroni, F., & Casapulla, C. (2021). Literature review of the in-plane behavior of masonry walls: Theoretical vs. experimental results. Materials, 14(11), 3063.

[5] Salmanpour, A. H., Mojsilović, N., & Schwartz, J. (2015). Displacement capacity of contemporary unreinforced masonry walls: an experimental study. Engineering Structures, 89, 1-16.

[6] CEN, EN 1996-1-1: 2005 Eurocode 6: Design of masonry structures—General rules for reinforced and unreinforced masonry structures. Management Centre: rue de Stassart, 36 B-1050 Brussels; 2005.

[7] CEN/TC250/SC8. Eurocode 8: Design of structures for earthquake resistance – Part 3: Assessment and retrofitting of buildings and bridges. Final Document EN1998-3 NEN SC8 PT3. Working draft 2018-05-22. European Committee for Standardization.

[8] CEN. EN 1998-1: 2004: Eurocode 8: Design of structures for earthquake resistance. Part 1: General rules, seismic actions and rules for buildings. Management Centre: rue de Stassart, 36 B-1050 Brussels; 2004.

[9] CEN, EN 1998-3: 2005: Eurocode 8. Design of Structures for Earthquake Resistance. Assessment and Retrofitting of Buildings. Management Centre: rue de Stassart, 36 B-1050 Brussels; 2005.

[10] Haach, V. G., Vasconcelos, G., & Lourenço, P. B. (2010). Experimental analysis of reinforced concrete block masonry walls subjected to in-plane cyclic loading.

[11] Bosiljkov, V. Z., Totoev, Y. Z., & Nichols, J. M. (2005). Shear modulus and stiffness of brickwork masonry: an experimental perspective. Structural Engineering and Mechanics, 20(1), 21-44.

[12] Dais, D., Sarhosis, V., Smyrou, E., & Bal, I. E. (2021). Seismic intervention options for multi-tiered Nepalese Pagodas: The case study of Jaisedewal temple. Engineering Failure Analysis, 123, 105262.

[13] Valente, M., & Milani, G. (2018). Damage assessment and partial failure mechanisms activation of historical masonry churches under seismic actions: three case studies in Mantua. Engineering Failure Analysis, 92, 495-519.

[14] Aref, A. J., & Dolatshahi, K. M. (2013). A three-dimensional cyclic meso-scale numerical procedure for simulation of unreinforced masonry structures. Computers & Structures, 120, 9-23.

[15] Guo, Y. T., Bompa, D. V., & Elghazouli, A. Y. (2022). Nonlinear numerical assessments for the in-plane response of historic masonry walls. Engineering Structures, 268, 114734.

[16] D'Altri, A. M., de Miranda, S., Castellazzi, G., & Sarhosis, V. (2018). A 3D detailed micro-model for the in-plane and out-of-plane numerical analysis of masonry panels. Computers & Structures, 206, 18-30.

[17] Kamrava, A. R., Najafgholipour, M. A., & Fathi, F. (2021). A Numerical Investigation on the In-Plane Behavior of Perforated Unreinforced Masonry Walls. Iranian Journal of Science and Technology, Transactions of Civil Engineering, 45(2), 545-560.

[18] Sarhosis, Vasilis, Katalin Bagi, José V. Lemos, and Gabriele Milani, eds. Computational modelling of masonry structures using the discrete element method. IGI Global, 2016.

[19] Pulatsu, B., Bretas, E. M., & Lourenco, P. B. (2016). Discrete element modeling of masonry structures: Validation and application.

[20] Tariq, H., Najafgholipour, M. A., Sarhosis, V., & Milani, G. (2023, January). In-plane strength of masonry wall panels: A comparison between design codes and high-fidelity models. In Structures (Vol. 47, pp. 1869-1899). Elsevier.

[21] Magenes, G., Morandi, P., Penna, A., & Ferrata, V. (2008). D 7.1 c Test results on the behaviour of masonry under static cyclic in plane lateral loads. Test Report, ESECMaSE Poject, University of Pavia, EURCENTRE, Italy.

[22] Haach, V. G., Vasconcelos, G., & Lourenço, P. B. (2010). Experimental analysis of reinforced concrete block masonry walls subjected to in-plane cyclic loading.

[23] Bosiljkov, V. Z., Totoev, Y. Z., & Nichols, J. M. (2005). Shear modulus and stiffness of brickwork masonry: an experimental perspective. Structural Engineering and Mechanics, 20(1), 21-44.

[24] Salmanpour, A. H., Mojsilovic, N., & Schwartz, J. (2013). Deformation capacity of unreinforced masonry walls subjected to in-plane loading: a state-of-the-art review. International Journal of Advanced Structural Engineering, 5(1), 1-12.

[25] Tomaževič, M., Lutman, M., & Bosiljkov, V. (2006). Robustness of hollow clay masonry units and seismic behaviour of masonry walls. Construction and Building Materials, 20(10), 1028-1039.